E12-06-114 Jeopardy Update:

Measurements of the electron-helicity dependent cross sections of deeply virtual Compton scattering in Hall A at 11 GeV

Spokespersons: A. Camsonne, C. Hyde, C. Muñoz Camacho and J. Roche

June 2019

Abstract

This is a Jeopardy update on experiment E12-06-114, originally approved by PAC30 (2006). Its beam-time was allocated by PAC38 (2011), who recommended a rating of A and the full 100 days requested. This experiment was furthered reviewed a 3$^{\text{rd}}$ time by PAC41 (2014) who classified 70 out of its 100 days as "High Impact". Since the most recent review, about half of the data approved for experiment E12-06-114 (50 days) were taken and analyzed. The remaining 50 days of E12-06-114 go now under review by PAC47 (2019). Our results from the first half of the experiment are ready for submission for publication and will be presented in this document. In addition to these results, we review our publications from 6 GeV Hall A experiment E07-007, as they pertain to the scientific case for the jeopardy proposal. We propose two scenarios to complete data taking for E12-06-114.

Contents

1 Hall A DVCS Experiment E12-06-114

1.1 Initial project

Experiment E12-06-114[1] was originally proposed as a follow-up to the successful pioneering experiment E00-110 [2]. Based on that first success, a full Generalized Parton Distributions (GPD) program with deep exclusive reactions in Hall A has been devoted to high precision measurements of deeply virtual exclusive (DVES) reactions cross sections. Indeed, GPD measurements at Jefferson Lab rely on the assumption that deep exclusive reactions are well described by their leading twist mechanism. Theoretically, this is true at high momentum transfer Q^2. The value of Q^2 at which this approximation is valid experimentally needs to be determined and the contributions of higher twist components to observables need to be quantified. The Q^2-dependence of cross sections is the only unambiguous way to separate higher twist contributions to Deeply Virtual Compton Scattering (DVCS) and other exclusive channels.

E12-06-114 experiment was approved by PAC30 with its beam-time allocated by PAC38. Its primary goal is to measure the Q^2-dependence of the DVCS and exclusive π^0 electroproduction cross sections, for different fixed values of the Bjorken variable x_B and momentum transfer to the nucleon t. By independently measuring the unpolarized cross section and the beam-helicity dependent cross section, E12-06-114 is able to separate the real and the imaginary parts of the DVCS amplitude. This was originally planned to be performed at three values of $x_B = 0.36$, 0.5 and 0.6 with at least a factor of 2 lever-arm in Q^2 at each value of x_B and t.

With a luminosity of up to 10^{38} cm^{-2}s^{-1} and by adjusting beam-time to each particular setting, cross sections can be measured with 3 to 5% statistical accuracy within a few days, even at high values of Q^2. High statistics allow fine binning, which is particularly useful because of the very rapid variations of the cross section[1]. Thanks to the well-understood acceptance of the Hall A High Resolution Spectrometer (HRS) and the simple and compact geometry of the DVCS calorimeter, the systematic uncertainties in the cross section measurements are around 4%. The high resolution of the HRS means that the kinematic variables will be very precisely determined, allowing an accurate study of the azimuthal dependence of the cross sections.

1.2 Progress of the field since the 2006 proposal

Hall A DVCS experiments E07-007 (proton) and E08-025 (deuterium) clearly demonstrated the importance and power of measurements of the incident-beam energy-dependence of deep virtual exclusive scattering (DVES) cross sections.

For deep virtual π^0 production, this is a conventional Rosenbluth separation of the cross sections for longitudinally and transversely polarized virtual photons. Our data [3, 4] confirmed the suspicion from previous Hall A and Hall B unseparated cross sections, that DVES π^0 production is dominated by the transverse cross section. On the one hand, this contradicts the QCD factorization theorem, which states that at sufficiently high Q^2, all deep virtual exclusive meson channels should be dominated by $d\sigma_L$. At the same time, the $d\sigma_T$ dominance confirmed (or at least supported) the conjecture by S. Liuti *et al.* [5] and S. Goloskokov & P. Kroll [6], that strong chiral symmetry breaking in the pion distribution amplitude (DA) leads to an effective factorization with $d\sigma_T$ sensitive to nucleon transversity GPDs.

We refer to the energy-dependent DVCS cross sections as a "generalized Rosenbluth Separation". At fixed (Q^2, x_B, t), the Bethe-Heitler (BH) and virtual Compton amplitudes have different

[1]Specifically the Bethe-Heitler part of the total cross-section

dependence on the incident-beam energies. Thus beam energy scans of the $(e, e'\gamma)$ cross section provides sensitivity to the real part of the [DVCS†BH] interference, that is otherwise only accessible via combining lepton and anti-lepton scattering.

A major theoretical advance for DVCS was carried out in 2014 by Braun *et al.* [7]. They developed a framework that allows to quantitatively account for kinematical power corrections of $\mathcal{O}(-t/Q^2)$ and $\mathcal{O}(M^2/Q^2)$ to the DVCS amplitude. These corrections turned out to be significant for JLab kinematics. While the DVCS scattering amplitude is a Lorentz invariant quantity, the deeply virtual scattering process nonetheless defines a preferred axis (light-cone axis) for describing the scattering process. At finite Q^2 and non-zero t, there is an ambiguity in defining this axis, though all definitions converge as $Q^2 \to \infty$ at fixed t. Belitsky et al. [8] decompose the DVCS amplitude in terms of photon-helicity states (λ,λ') where the light-cone axis is defined in the plane of the four-vectors q and P. This leads to a given set of GPD convolutions $\mathcal{F}_{\lambda\lambda'}$ called Compton Form Factors (CFFs) that parametrize the DVCS cross section. Braun *et al.* [7] proposed an alternative decomposition which defines the light cone axis in the plane formed by q and q', which turned out to be more convenient to account for kinematical power corrections of $\mathcal{O}(-t/Q^2)$ and $\mathcal{O}(M^2/Q^2)$. The bulk of these corrections can be included by rewriting the CFFs $\mathcal{F}_{\lambda\lambda'}$ in terms of the Braun CFFs $\mathbb{F}_{\lambda\lambda'}$ using the following map [7]:

$$\mathcal{F}_{++} = \mathbb{F}_{++} + \tfrac{\chi}{2}\left[\mathbb{F}_{++} + \mathbb{F}_{-+}\right] - \chi_0 \mathbb{F}_{0+} \,, \quad (1)$$

$$\mathcal{F}_{-+} = \mathbb{F}_{-+} + \tfrac{\chi}{2}\left[\mathbb{F}_{++} + \mathbb{F}_{-+}\right] - \chi_0 \mathbb{F}_{0+} \,, \quad (2)$$

$$\mathcal{F}_{0+} = -(1+\chi)\mathbb{F}_{0+} + \chi_0\left[\mathbb{F}_{++} + \mathbb{F}_{-+}\right] \,, \quad (3)$$

where kinematic parameters χ_0 and χ are defined as follows (Eq. 48 of Ref [7]):

$$\chi_0 = \frac{\sqrt{2}Q\widetilde{K}}{\sqrt{1+\epsilon^2}(Q^2+t)} \propto \frac{\sqrt{t_{min}-t}}{Q} \,, \quad (4)$$

$$\chi = \frac{Q^2 - t + 2x_B t}{\sqrt{1+\epsilon^2}(Q^2+t)} - 1 \propto \frac{t_{min}-t}{Q^2} \,. \quad (5)$$

Within the $\mathbb{F}_{\mu\nu}$-parameterization, the leading-twist and leading-order approximation consists in keeping $\mathbb{F}_{++}$ and neglecting both $\mathbb{F}_{0+}$ and $\mathbb{F}_{-+}$. Nevertheless, as a consequence of Eq. 2 and 3, $\mathcal{F}_{0+}$ and $\mathcal{F}_{-+}$ are no longer equal to zero since proportional to $\mathbb{F}_{++}$. The functions that can be extracted from data to describe the three dimensional structure of the nucleon become:

$$\mathcal{F}_{++} = (1+\frac{\chi}{2})\mathbb{F}_{++}, \qquad \mathcal{F}_{0+} = \chi_0\mathbb{F}_{++}, \qquad \mathcal{F}_{-+} = \frac{\chi}{2}\mathbb{F}_{++}. \quad (6)$$

A numerical application gives χ_0 =0.25 and χ =0.06 for Q^2=2 GeV^2, x_B=0.36 and $t = -0.24$ GeV^2. Considering the large size of the parameters χ_0 and χ, these kinematical power corrections cannot be neglected in precision DVCS phenomenology, in particular in order to separate the DVCS-BH interference and DVCS^2 contributions. Indeed, when the beam energy changes, not only do the contributions of the DVCS-BH interference and DVCS^2 terms change but also the polarization of the virtual photon changes, thereby modifying the weight of the different helicity amplitudes.

Fig. 1 shows the beam helicity-dependent and helicity-independent cross sections measured in one kinematic bin of E07-007 [9], at two different values of the incident beam energy. Neglecting the (logarithmic) Q^2–evolution of the CFFs between 1.5 to 2 GeV^2, a combined fit of all the data at constant x_B and t is performed. For each $-t$ bin, this fit includes the helicity-dependent and

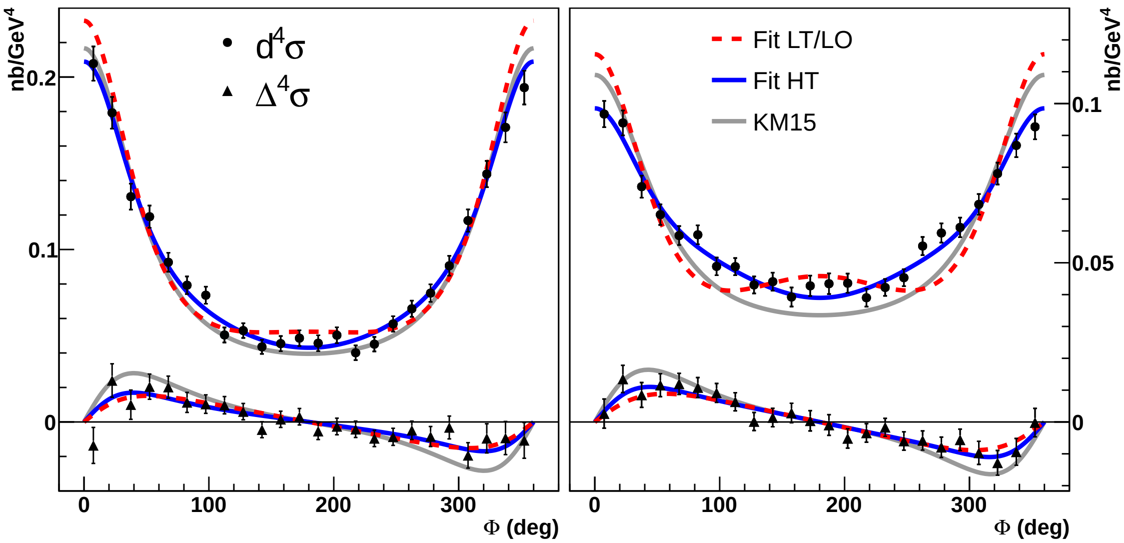

Fig. 1: **Beam helicity-dependent ($\Delta^4\sigma$) and helicity-independent ($d^4\sigma$) cross sections at Q^2=1.75 GeV^2, x_B=0.36, and $t = -0.30$ GeV^2.** The beam energies are E^{beam}=4.455 GeV (left) and E^{beam}=5.55 GeV (right). Dashed lines represent the result of the LT/LO fit with $\mathbb{H}_{++}$,$\mathbb{E}_{++}$,$\widetilde{\mathbb{H}}_{++}$ and $\widetilde{\mathbb{E}}_{++}$. Solid lines show the result of the HT fit with $\mathbb{H}_{++}$,$\widetilde{\mathbb{H}}_{++}$,$\mathbb{H}_{0+}$, and $\widetilde{\mathbb{H}}_{0+}$. Curves for the NLO fit ($\mathbb{H}_{++}$,$\widetilde{\mathbb{H}}_{++}$,$\mathbb{H}_{-+}$, and $\widetilde{\mathbb{H}}_{-+}$) overlap with the HT fit and are not shown. Results from the KM15 [10, 11] fit to previously published DVCS data is also presented.

helicity-independent cross sections at 2 values of beam energy and all 3 values of Q^2. The leading-twist and leading-order (LO/LT) fit is shown in Fig. 1 for $t = -0.30$ GeV^2, in which the free parameters are the real and imaginary parts of $\mathbb{H}_{++}$, $\widetilde{\mathbb{H}}_{++}$, $\mathbb{E}_{++}$ and $\widetilde{\mathbb{E}}_{++}$. This fit reproduces very poorly the angular distribution of the data yielding a value of $\chi^2/ndf = 415/208$. Indeed, the strong enhancement of the $\cos\phi$-harmonics in the DVCS^2 amplitude originated by the large size of χ_0 translates into the bump in the dashed line around ϕ=180° for E^{beam}=5.550 GeV. Two additional fits were performed including either (a) $\{\mathbb{H}_{0+}, \widetilde{\mathbb{H}}_{0+}\}$ to include genuine twist-3 contributions or (b) $\{\mathbb{H}_{-+}, \widetilde{\mathbb{H}}_{-+}\}$ to include gluon-transversity GPD contributions. In both of these latter fits $\mathbb{E}_{++}$ and $\widetilde{\mathbb{E}}_{++}$ were set to zero, thus keeping constant the number of free parameters. The fit to the data is much better ($\chi^2/ndf = 210/208$) for both the higher-twist (HT) or the next-to-leading order (NLO) scenarios than for the LO/LT case. This conclusion also holds for the lower $-t$ bins, as summarized in Tab. 1. These results from 2017 including the kinematical power corrections recently calculated for DVCS demonstrate that the leading twist approximation is no longer sufficient to describe accurate DVCS data at JLab.

A new proposal was approved by PAC40 to extend this program and exploit the $\epsilon-$dependence of the cross section in order to separate the pure DVCS^2 cross section from the DVCS interference with the BH amplitude. This experiment (E12-13-010 [12]) was proposed in Hall C because of the requirement to detect scattered electron momenta higher than the Hall A HRS limitation of 4 GeV/c. Hall C E12-13-010 plans to add different energy settings at kinematics measured in Hall A during E12-06-114. The Hall C experiment proposal assumed all approved kinematics in Hall A would be acquired so as to allow the (generalized) Rosenbluth separation of DVCS and π^0.

With its higher momentum reach of up to 7.4 GeV, the Hall C High Momentum Spectrometer (HMS) will allow an L/T separation of the DVCS and π^0 exclusive cross sections to be performed. In

Fit Description:	LO/LT	Higher Twist	NLO
Helicity States:	++	++/0+	++/−+
$t = -0.18$ GeV^2	250	204	206
$t = -0.24$ GeV^2	367	206	208
$t = -0.30$ GeV^2	415	186	190

Tab. 1: Values of χ^2 ($ndf = 208$) obtained (Fig. 1) in the leading-order, leading-twist (++); higher-twist (++/0+); and next-to-leading-order (++/−+) scenarios.

addition, the kinematic coverage can be expanded to higher Q^2 and smaller values of x_B compared with those currently approved in Hall A.

1.3 2014 and 2016 data taking and results

From Fall 2014 through Fall 2016, during the accelerator and Hall A commissioning of the 12 GeV Upgrade, the Hall A DVCS collaboration acquired 50% of the approved 100 PAC days of beam-time for experiment E12-06-114 [1]. The kinematic reach of these measurements is illustrated in Fig. 2. In order to complete this "phase-one" of E12-06-114, within the available beam-time, the following compromises were made:

- The intended beam-time of each of the four settings (in green) centered at $x_B = 0.48$ was reduced;
- Approved kinematic points centered at $x_B = 0.60$ and $Q^2 = 6.82$ & 9.0 GeV^2 were omitted.

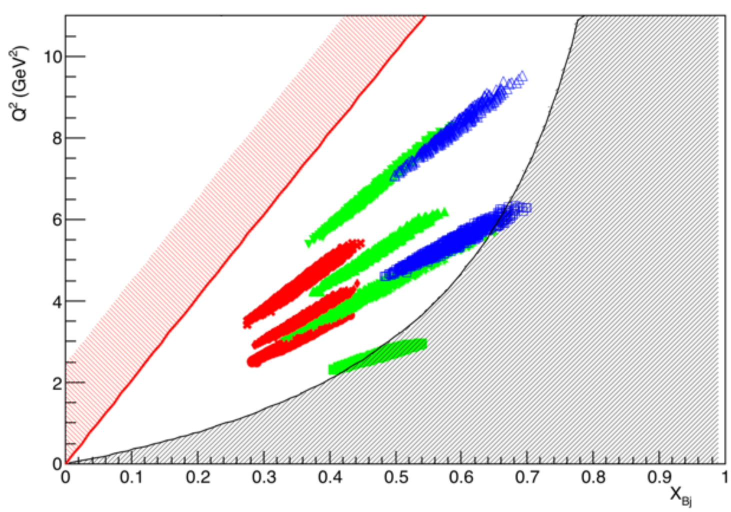

Fig. 2: DVCS Kinematics, 2014-2016. The incident beam energies ranged from 4.5 GeV to 11 GeV (2-5 pass). The kinematics are shifted somewhat from the original proposal, due to limitations of the HRS-Left spectrometer, and variations in the CEBAF energy per pass. The lower exclusion zone is $W^2 \leq 4$ GeV^2, the upper exclusion zone is the kinematic limit for an incident energy of 11 GeV.

The DVCS data were acquired via the H$(e, e'\gamma)p$ channel, with the scattered electron detected in the Hall A HRS-Left spectrometer, the γ-ray detected in a 208-element PbF_2 calorimeter, and the exclusive proton reconstructed by missing mass. We measured the deep virtual exclusive π^0 channel, H$(e, e'\gamma\gamma)p$, in parallel, with both photons in the PbF_2 calorimeter.

Figure 3 shows a typical $ep \to e\gamma X$ missing mass squared distribution. Accidental coincidences are subtracted by measuring the number of coincidences in a time window of equal size but out-of-time with the electron trigger. The contamination due to π^0 decays that yield one photon in the calorimeter is calculated (and then subtracted) by measuring the number of π^0 detected and computing in a Monte-Carlo simulation the probability of missing one of the photons when each π^0 decays along a different angle with respect to its momentum in its center-of-mass frame.

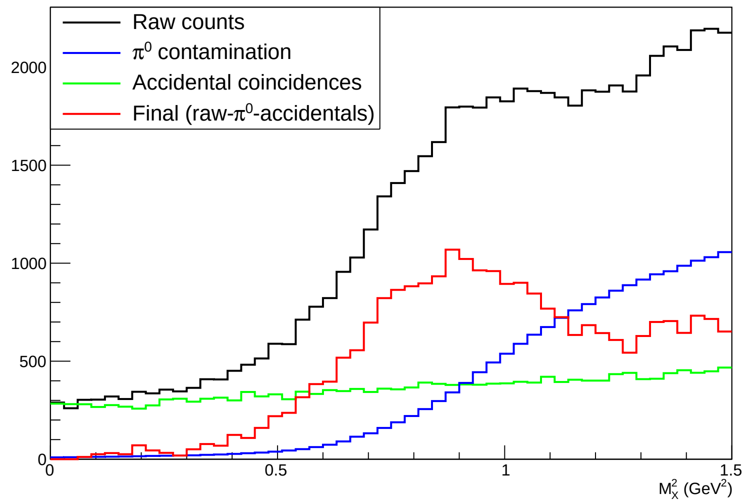

Fig. 3: Missing mass squared of the $ep \to e\gamma X$ reaction for the setting at $x_B = 0.48$ and $Q^2 = 2.7$ GeV^2, integrated over t and ϕ. Raw data is shown in black. The subtraction of the accidental contribution (green) and photons from π^0 decays (blue) yields the red histogram.

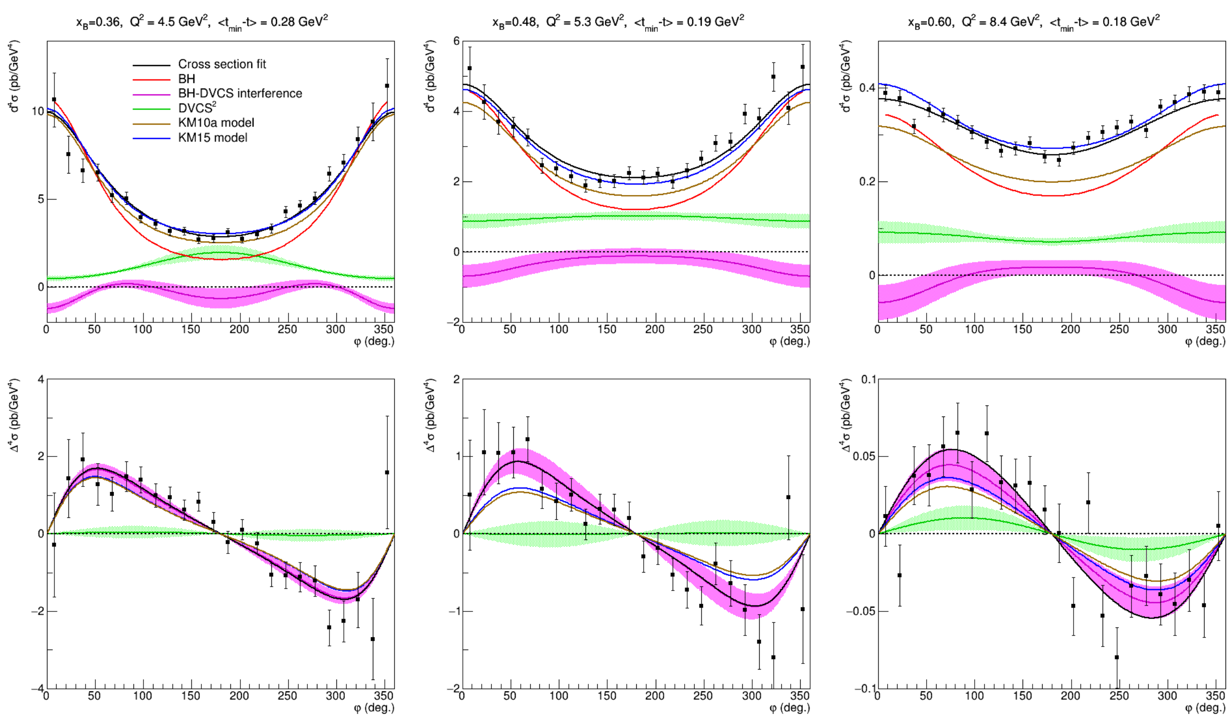

Fig. 4: Helicity-independent (top) and helicity-dependent (bottom) DVCS cross section at $x_B = 0.36$ (left), $x_B = 0.48$ (center) and $x_B = 0.60$ (right) for the value of Q^2 and t indicated on the top of each figure. Black curves show the higher-twist fits (indistinguishable from the LO/LT or NLO fits) in the BMMP formalism. The BH cross section is shown in red. The contribution from the BH-DVCS interference is shown by the magenta bands (HT fit), whereas the contribution from the DVCS^2 term is indicated by the green bands (HT fit). Models KM10a and KM15 [13] are shown in brown and blue respectively.

Figure 4 shows a sample of the cross sections measured at each of the x_B settings. The azimuthal dependence of the cross section is fitted using the BMMP formalism [7] and the BH-DVCS interference and DVCS^2 contributions are shown along with the BH cross section. The free parameters of the fit are the different CFFs. All kinematic bins at constant x_B and t are fitted simultaneously and the fit is performed in different scenarios. The leading-order and leading-twist (LO/LT) fit includes $\mathbb{H}_{++}$, $\widetilde{\mathbb{H}}_{++}$, $\mathbb{E}_{++}$ and $\widetilde{\mathbb{E}}_{++}$. The higher-twist (HT) fit includes $\mathbb{H}_{++}$, $\widetilde{\mathbb{H}}_{++}$, $\mathbb{H}_{0+}$ and $\widetilde{\mathbb{H}}_{0+}$. The next-to-leading order (NLO) fit includes $\mathbb{H}_{++}$, $\widetilde{\mathbb{H}}_{++}$, $\mathbb{H}_{-+}$ and $\widetilde{\mathbb{H}}_{-+}$. All fits yield a similar quality as evidenced by their χ^2/ndf reported in Tab. 2 and overlay in Fig. 4. However, the contributions of the BH-DVCS interference and the DVCS^2 terms depend significantly on which scenario the fit is performed (LO/LT, HT or NLO). Fig. 4 shows their contribution in the HT scenario.

x_B	LO/LT	HT	NLO
0.36	1.63	1.49	1.49
0.48	1.49	1.35	1.36
0.60	1.62	1.31	1.33

Tab. 2: Values of χ^2/ndf for the leading-order/leading-twist (LO/LT), higher-twist (HT) and next-to-leading-order (NLO) fits of the helicity-dependent and helicity-independent cross sections at each value of x_B.

One major conclusion from this "phase-one" of E12-06-114 is the impossibility to clearly distinguish the LO/LT fit from their HT or NLO counterparts. Measurements at the same Q^2 and x_B but different beam energies is essential for that, as results from E07-007 [3] showed. This motivated the approved program of DVCS measurements in Hall C [12].

2 Experiment E12-06-114 Jeopardy Proposal

2.1 The Hall A scenario

Because of the reduced beam-time scheduled up to date for E12-06-114, not all of the planned settings could be acquired. In addition, the frequent change of the linac energy over the running period of the experiment (2014–2016) prevented us to add more statistics to settings that were initiated in a previous Spring or Fall run of CEBAF. This resulted in:

- Two of the time-consuming measurements at $x_B = 0.60$ were not taken at all. Only 2 out of the 4 points in Q^2 at constant $x_B = 0.60$ could be done;
- The settings initially planned at $x_B = 0.5$ were slightly shifted to $x_B = 0.48$. All four setting at this x_B were acquired, but with a significant reduction in the statistics with respect to the original proposal (up to 50% in some of the settings).

Figure 5 shows the Q^2-dependence of the leading-twist CFF combination $\mathcal{I}m\,\mathcal{C}^I$, extracted from the amplitude of the $\sin\phi$ term in the helicity-dependent cross section. Data are plotted at constant x_B and t. The 2 missing values (with respect to the original proposal) at $x_B = 0.60$ and the larger statistical uncertainties at $x_B = 0.48$ reflect the points mentioned above.

While kinematics at $x_B = 0.36$ show no dependence with Q^2, at higher values of x_B a strong statement cannot be made due to the size of the uncertainties or the lack of data points. The remaining 50 days of approved beam-time yet to be scheduled will allow to reduce the uncertainties at $x_B = 0.48$ and add 2 more points at $x_B = 0.60$ as planned in the original proposal.

We describe below an alternative scenario that would address some of these issues by running the rest of the experiment in Hall C using the Neutral Particle Spectrometer facility. By using the higher luminosity allowed by the sweeping magnet, the larger acceptance and better resolution of the

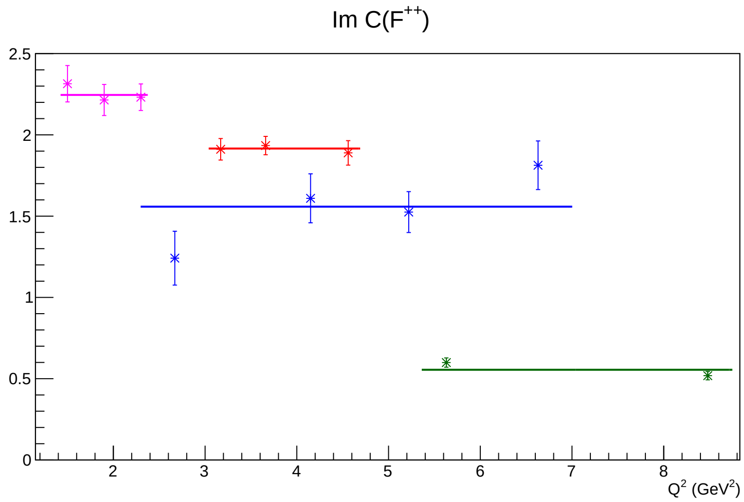

Fig. 5: Values of $\mathcal{I}\mathrm{m}\,\mathcal{C}^I$ as a function of Q^2 at constant t and $x_B = 0.36$ (red), $x_B = 0.48$ (blue) and $x_B = 0.6$ (green). Previous results [2] at $x_B = 0.36$, but smaller value of t are shown in magenta.

$PbWO_4$ calorimeter and the larger momentum reach of the Hall C High Momentum Spectrometer (HMS), we could reduce the number of beam-days to 30 as described in the following.

2.2 The Hall C Neutral Particle Spectrometer scenario

Hall C DVCS experiment E12-13-010 is approved to extend the Q^2 range of the Hall A E12-06-114 measurements, and to provide multiple beam energy measurements at fixed (x_B, Q^2). The new Neutral Particle Spectrometer (NPS) rides on the SHMS carriage, and includes a 36×30 array of 2×2 cm^2 $PbWO_4$ crystals with a 0.6 Tm sweep magnet. The sweep magnet reduces the accidental rate in the calorimeter by a factor of 10. Combined with scintillating $PbWO_4$ crystals, this will deliver higher photon resolution at higher luminosity than the Hall A configuration. Transferring this jeopardy proposal to Hall C will have the following benefits:

- The greater range of the Hall C HMS spectrometer will enable beam energy-dependent measurements at higher Q^2 than with the existing mix of Hall A/C measurements;
- The NPS-HMS combination enables measurements close to the kinematic limit, with the calorimeter at very small angles;
- The reduced background in the γ-calorimeter enables running at higher luminosity, which makes more efficient use of the beam-time.

The proposed jeopardy kinematics are listed in Tab. 3. Exact kinematics will be adjusted depending upon the standard linac energy at the time of the run. These kinematics are chosen to maximize the number of (Q^2, x_B) settings at which we will obtain data with at least two beam energy values. **This will allow both the L/T separation of the exclusive π^0 cross sections and the generalized Rosenbluth Separation of DVCS**. Combining the Jeopardy kinematics with previously taken Hall A E12-06-114 and approved Hall C NPS E12-13-010 settings (Tab. 4) we will obtain the following energy scans:

- $x_B = 0.48$: $Q^2 = 3.4,\ 4.3,\ \&\ 5.3$ GeV^2, 4 and 5 pass beam
- $x_B = 0.60$: $Q^2 = 5.5,\ 6.8,\ \&\ 8.4$ GeV^2, 4 and 5 pass beam

Figure 6 shows the Q^2 dependence of settings proposed, together with those already collected in Hall A and those already approved in Hall C at $x_B = 0.48$ and $x_B = 0.60$. Estimated cross sections for the proposed jeopardy kinematics are shown in Fig. 7. Beam-time for each of the settings has been calculated to match the statistical accuracy of previously approved settings, based on the KM15 global fit [13] of DVCS data, which reproduces well the cross sections measured in the "phase-one" of E12-06-114. The total beam-time required is 30 days.

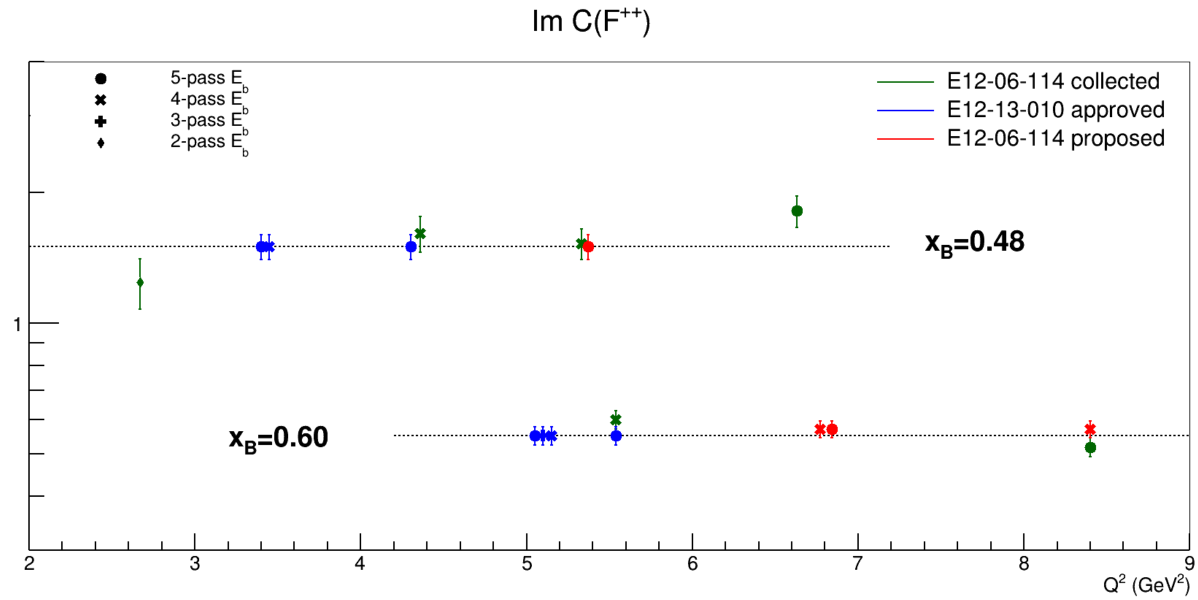

Fig. 6: Q^2-dependence of settings at $x_B = 0.48$ and $x_B = 0.60$. Green symbols indicate the data already acquired in the 50 days of beam taken in Hall A for E12-06-114. Blue points are the settings already approved in Hall C for experiment E12-13-010. The new settings proposed here to complete the Hall A E12-06-114 using the NPS facility in Hall C are indicated in red. The different marker styles show the different beam energy of each setting as described in the top-left legend.

Variable \ Setting	Units	Kin48_J1	Kin60_J1	Kin60_J2	Kin60_J3
x_B		0.480		0.600	
Q^2	GeV^2	5.334	6.822		8.40
Beam Energy	GeV	10.617	8.517	10.617	8.517
HMS (e^-)	GeV/c	4.696	2.458	4.558	1.057
HMS (θ_e)	deg	-18.83	-33.17	-21.64	-57.77
NPS (γ-Calo)	deg	13.79	11.76	14.76	6.41
D(Calo)	m	3.0	3.0	3.0	4.0
Luminosity	10^{37}/cm^2/sec	7.5	7.5	7.5	13
Beam Current	μA	30	30	30	50
PAC Days	**Day**	**3**	**8**	**7**	**12**

Tab. 3: Jeopardy Kinematics for Hall C — NPS running. HMS and NPS values are the nominal central values. Negative angles are beam-left, positive angles are beam-right. The total beam-time required to run these settings is 30 days.

Variable \ Setting	Units	NPS48_1	NPS48_2	NPS48_3	NPS60_1
x_B		0.480			0.60
Q^2	GeV^2	3.40		4.36	5.54
Beam Energy	GeV	8.517	10.617	10.617	10.617
HMS (e^-)	GeV/c	4.742	6.842	5.771	5.696
HMS (θ_e)	deg	-16.68	-12.42	-15.38	-17.41
NPS (γ-Calo)	deg	18.91	20.51	16.82	18.20
D(Calo)	m	3.0	3.0	3.0	3.0

Tab. 4: Select DVCS kinematics from approved Hall C, NPS E13-12-010. These settings are adjusted slightly from the original proposal, to better align with the Hall A data, in view of the revised linac energies.

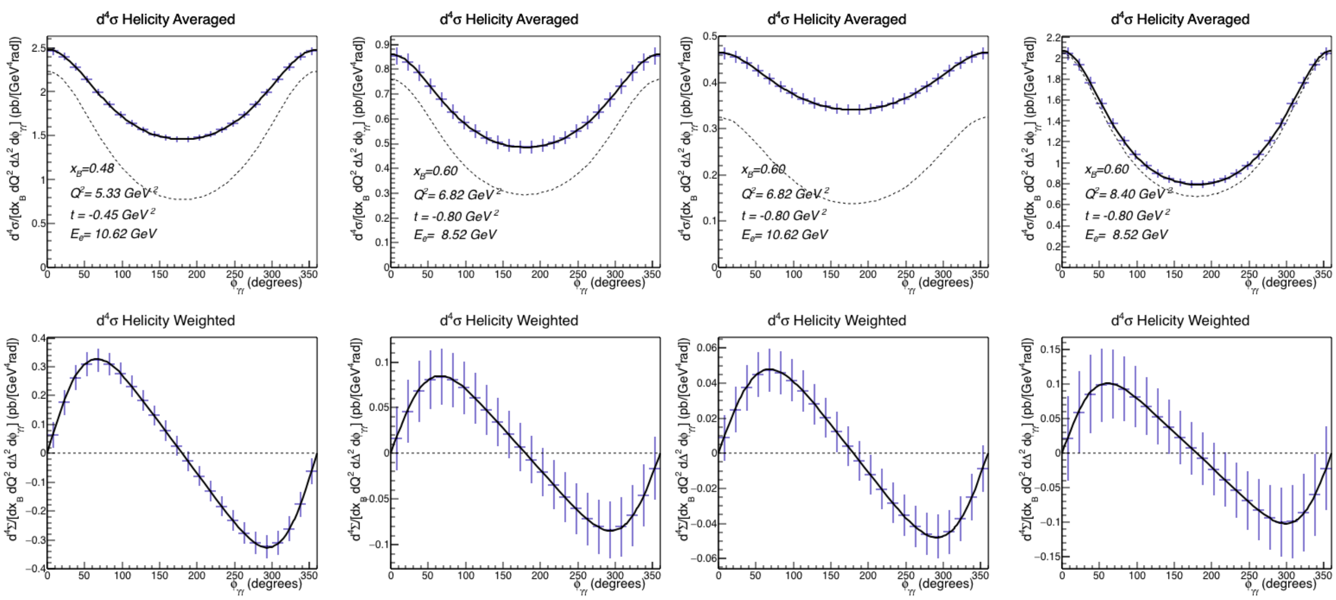

Fig. 7: Estimated cross sections and statistical uncertainties for settings Kin48_J1 and Kin60_J1–J3 (left to right). For each setting, only one t-value is shown. Each cross section is averaged over the HMS acceptance and a bin of $\Delta t = 0.05$ GeV^2. For Kin60_J3, the $t-$bin width is 0.10 GeV^2. The cross sections are obtained from the KM15 model [13], and the dashed lines are the pure Bethe-Heitler cross sections.

3 Summary

E12-06-114 was approved with A rating by PAC30 (2006), 100 days of beam-time were allocated by PAC 38 (2011), 70 of them were categorized as 'High Impact' by PAC41 (2014). During 2014–2016 E12-06-114 was scheduled to run 50 days out of the 100 days approved. The remaining 50 days are still not scheduled. We have presented in this document an update of recent developments in the field. In particular, recent results and theoretical work have shown that:

- The beam-energy dependence of the DVCS cross section is a powerful tool to further investigate the reaction mechanism of DVCS;
- Power corrections of $\mathcal{O}(-t/Q^2)$ and $\mathcal{O}(M/Q^2)$ are important at Jefferson Lab kinematics;
- Precise measurements of absolute cross sections at well-defined kinematics is the best way to

understand higher twist and/or higher order corrections to the DVCS process;

- Neutral pion electroproduction is dominated by its transverse cross section, which can in a unique way probe the transversity GPDs of the nucleon. An L/T separation of this channel is therefore extremely interesting.

In addition to these physics results, a new facility with higher resolution and luminosity is being developed in Hall C (the Neutral Particle Spectrometer, NPS). A DVCS experiment (E12-010-013) was approved by PAC40 (2010) with A rating to run using this facility. The experiment may be able to be scheduled as soon as 2021. On the other hand, the PbF_2 calorimeter used in Hall A for the initial run of E12-06-114 is still available and the remaining beam-time can be scheduled in Hall A anytime.

We have presented herein the physics case for running the remaining 50 days in Hall A, as well as the option of running the remaining time in Hall C. The latter would lead to a reduced beam time of 30 days, but it will require the availability of the NPS facility.

References

1. J. Roche *et al.*, (2006), Measurements of the electron-helicity dependent cross-sections of deeply virtual compton scattering with CEBAF at 12-GeV, arXiv:nucl-ex/0609015 [nucl-ex] .

2. M. Defurne *et al.* (Jefferson Lab Hall A), Phys. Rev. **C92**, 055202 (2015), arXiv:1504.05453 [nucl-ex] .

3. M. Defurne *et al.* (Jefferson Lab Hall A), Phys. Rev. Lett. **117**, 262001 (2016).

4. M. Mazouz *et al.* (Jefferson Lab Hall A), Phys. Rev. Lett. **118**, 222002 (2017).

5. S. Ahmad, G. R. Goldstein, and S. Liuti, Phys. Rev. **D79**, 054014 (2009).

6. S. Goloskokov and P. Kroll, Eur.Phys.J. **A47**, 112 (2011), arXiv:1106.4897 [hep-ph] .

7. V. M. Braun, A. N. Manashov, D. Muller, and B. M. Pirnay, Phys. Rev. **D89**, 074022 (2014).

8. A. V. Belitsky, D. Muller, and Y. Ji, Nucl. Phys. **B878**, 214 (2014).

9. M. Defurne *et al.*, Nature Commun. **8**, 1408 (2017), arXiv:1703.09442 [hep-ex] .

10. K. Kumericki and D. Muller, Nucl.Phys. **B841**, 1 (2010), arXiv:0904.0458 [hep-ph] .

11. K. Kumericki, S. Liuti, and H. Moutarde, Eur. Phys. J. **A52**, 157 (2016).

12. C. Muñoz Camacho, T. Horn, C. Hyde, R. Paremuzyan, J. Roche *et al.*, JLab proposal (2013), Exclusive Deeply Virtual Compton and Neutral Pion Cross-Section Measurements in Hall C, `https://www.jlab.org/exp_prog/proposals/13/PR12-13-010.pdf`.

13. K. Kumericki and D. Mueller, *Proceedings, 6th International Conference on Physics Opportunities at an ElecTron-Ion Collider (POETIC 2015): Palaiseau, France, September 7-11, 2015*, EPJ Web Conf. **112**, 01012 (2016), arXiv:1512.09014 [hep-ph] .